

# Liquid-Liquid Phase Split in Ionic Liquid + Toluene Mixtures Induced by CO<sub>2</sub>

Roberto I. Canales and Joan F. Brennecke

Dept. of Chemical and Biomolecular Engineering, University of Notre Dame, Notre Dame, IN 46556

DOI 10.1002/aic.14850

Published online August 7, 2015 in Wiley Online Library (wileyonlinelibrary.com)

High pressure carbon dioxide was dissolved in ionic liquid + toluene mixtures to obtain the conditions of pressure and composition where a liquid-liquid phase split occurs at constant temperature. Ionic liquids (ILs) with four different cations paired with the bis(trifluoromethylsulfonyl)imide ([Tf<sub>2</sub>N]<sup>−</sup>) anion were selected: 1-hexyl-3-methylimidazolium ([hmim]<sup>+</sup>), 1-hexyl-3-methylpyridinium ([hmpy]<sup>+</sup>), triethyloctylphosphonium ([P<sub>2228</sub>]<sup>+</sup>), and tetradecyltriethylphosphonium ([P<sub>6614</sub>]<sup>+</sup>). The solubility of CO<sub>2</sub> was measured in the liquid mixtures at temperatures between 298 and 333 K and at pressures up to 8 MPa, or until the second liquid phase appeared, for initial liquid phase compositions of 0.30, 0.50, and 0.70 mole fraction of IL. Ternary isotherms were compared with the binary solubility of CO<sub>2</sub> in each IL and pure toluene. The lowest pressure for separating toluene in a second liquid phase was achieved by decreasing the temperature of the system, increasing the amount of toluene in the initial liquid mixture and using [hmim][Tf<sub>2</sub>N]. © 2015 American Institute of Chemical Engineers *AIChE J.* 61: 2968–2976, 2015

**Keywords:** ionic liquids, phase equilibrium, separation techniques

## Introduction

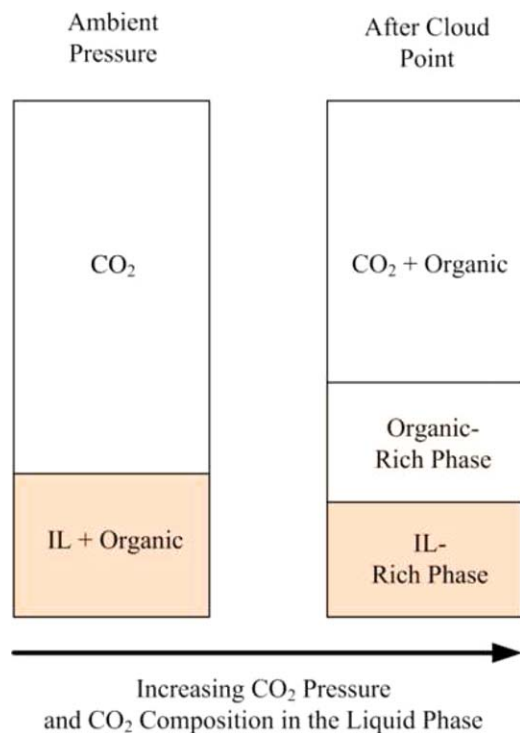
Ionic liquids (ILs) are salts extensively studied in recent years due to their interesting properties, including very low vapor pressure, high thermal stability, and wide liquid range, many of which include temperatures below 373 K.<sup>1</sup> Additionally, these compounds have adjustable physical and chemical properties. Given the large number of potential combinations of anion and cation,<sup>2</sup> this confers on them great versatility in being applied in a large number of specific processes. The literature describes multiple applications of ILs in separations; for example, in aqueous biphasic systems<sup>3</sup> for extracting conventional salts, amino acids, polymers, metals, or organic compounds from water; in liquid-liquid extractions for obtaining metal ions<sup>4–10</sup> or distributing organic compounds into two immiscible liquid phases<sup>11–14</sup>; for CO<sub>2</sub> capture from industrial gas streams<sup>15,16</sup>; and for separating compounds which form azeotropic mixtures.<sup>17</sup> The attractiveness of ILs in many of these applications coincides with their low volatility; thus, volatile solvents commonly used in separation processes can be replaced, in order to decrease vapor emissions to the environment.

CO<sub>2</sub>, a well-known solvent for extraction under supercritical conditions,<sup>18</sup> has been studied in conjunction with ILs. In the first report of this kind, Blanchard et al.<sup>19</sup> mixed naphthalene with [bmim][PF<sub>6</sub>] and utilized supercritical CO<sub>2</sub> for extracting the dissolved solid from the liquid phase. After the extraction, no IL was detected in the supercritical phase

and CO<sub>2</sub> could be easily separated from the naphthalene by depressurization, obtaining a solvent-free solute. Moreover, the same procedure has been used for extracting several organic solids and liquids<sup>20</sup> from the IL phase, demonstrating its general applicability. Following the idea of using high pressure CO<sub>2</sub>, Scurto et al.<sup>21</sup> proposed a new separation involving CO<sub>2</sub> and ILs applying the method depicted in Figure 1. In that work, an organic compound was mixed with an IL, forming a single liquid phase. Then, high pressure CO<sub>2</sub> was added to the system and solubilized in the liquid mixture until a second liquid phase appeared forming an IL-rich phase and an organic-rich phase, that is, a LV → LLV transition is observed. This is possibly due to the high solubility of CO<sub>2</sub> in ILs<sup>22–25</sup> and the antisolvent activity of this gas in decreasing the organic + IL interactions in the liquid phase.<sup>26</sup> The temperature, pressure, and composition of CO<sub>2</sub> where the phase split occurs, is called the “cloud point.” If more CO<sub>2</sub> is added after the cloud point and the pressure of the system is increased, the second liquid phase can disappear, resulting in only two phases, a liquid phase containing the three components and a supercritical phase composed of the CO<sub>2</sub> + organic mixture. The LLV → LV transition that is observed is called the “merging point.” This methodology has been applied for extracting water<sup>27</sup> and several organic compounds<sup>26,28</sup> from hydrophobic and hydrophilic ILs, and even for separating organic compounds from surfactants.<sup>29</sup> Also, composition analysis of the three phases for liquid-liquid-vapor equilibrium,<sup>28,30–32</sup> bubble and dew points,<sup>33–35</sup> and the observation of additional phase transitions, by changing the pressure of constant composition and temperature mixtures,<sup>36,37</sup> have been studied for several ILs + organic + CO<sub>2</sub> systems in literature. Most of these ternary systems involve polar organic compounds, opening the opportunity for

Additional Supporting Information may be found in the online version of this article.

Correspondence concerning this article should be addressed to J. F. Brennecke at jfb@nd.edu.



**Figure 1. Phase split of an organic + ionic liquid mixture induced by CO<sub>2</sub>.**

[Color figure can be viewed in the online issue, which is available at [wileyonlinelibrary.com](http://wileyonlinelibrary.com).]

describing the phase equilibrium of mixtures of CO<sub>2</sub> and ILs with nonpolar aliphatic, aromatic, and cyclic hydrocarbons.

The objective of this work is to measure the solubility of CO<sub>2</sub> in IL + toluene mixtures at 298, 313, and 333 K and up to 8 MPa using three different families of ILs (imidazolium, pyridinium, and phosphonium cation based). Conditions of pressure and temperature at which the cloud point is observed are determined, following the procedure described by Scurto et al.<sup>21</sup> Molar volumes of the mixtures are determined in order to analyze the correlation of volume expansion with CO<sub>2</sub> solubility and the appearance of cloud points. This work provides new phase equilibrium data for CO<sub>2</sub> + IL and CO<sub>2</sub> + toluene + ILs systems that may be useful in designing separation systems for even more complex systems involving hydrocarbons or hydrophobic compounds.

## Experimental Methods

### Materials

[hmim][Tf<sub>2</sub>N] was purchased from Merck. [hmpy][Tf<sub>2</sub>N], [P<sub>2228</sub>][Tf<sub>2</sub>N], and [P<sub>66614</sub>][Tf<sub>2</sub>N] were synthesized in our laboratory. Structures and purities of ILs used in this work are depicted in Table 1. The purity and full characterization of the synthesized ILs was determined by <sup>1</sup>H and <sup>13</sup>C NMR spectroscopy and thermogravimetric analysis. [hmpy][Tf<sub>2</sub>N] was synthesized by mixing 3-methylpyridine (Sigma-Aldrich, purity ≥ 0.99 mass fraction) with an excess of 1-bromohexane (Sigma-Aldrich, purity ≥ 0.98 mass fraction) in toluene to form 1-hexyl-3-methylpyridinium bromide ([hmpy][Br]). This first product was washed with *n*-hexane and diethyl ether. Then, [hmpy][Br] dissolved in water was mixed with lithium bis(trifluoromethylsulfonyl)imide (LiTf<sub>2</sub>N, 3M-Fluorad, purity ≥ 0.995 mass fraction) obtaining

[hmpy][Tf<sub>2</sub>N] which is washed with water to remove the lithium bromide. For synthesizing [P<sub>2228</sub>][Tf<sub>2</sub>N], triethylphosphine (Sigma-Aldrich, purity ≥ 0.99 mass fraction) is reacted with octylbromide (Sigma-Aldrich, purity ≥ 0.99 mass fraction) in acetonitrile to form [P<sub>2228</sub>][Br]. Significant care must be taken in handling triethylphosphine as it is highly flammable, pyrophoric, and corrosive. The product is washed with hexanes. Then, the same procedure of adding LiTf<sub>2</sub>N to the bromide is performed to obtain [P<sub>2228</sub>][Tf<sub>2</sub>N]. [P<sub>66614</sub>][Tf<sub>2</sub>N] was synthesized following the procedures shown elsewhere.<sup>25</sup> All ILs are placed under vacuum for at least 12 h at 333 K to obtain a water concentration below 0.0006 mass fraction. Water content was measured by Karl Fischer Coulometry (Metrohm 831). The observed [Br]<sup>−</sup> content in the ILs synthesized in our laboratory is normally below 10 ppm. This concentration is measured by ion chromatography. Toluene (anhydrous, purity > 0.998 mass fraction) was purchased from Acros Organics and CO<sub>2</sub> (purity > 0.998 mass fraction) from Mittler Supply, South Bend, IN.

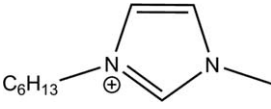

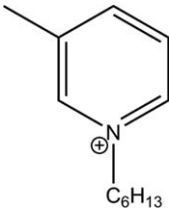
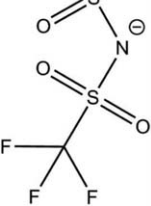
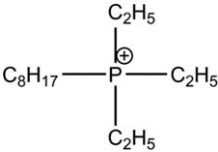
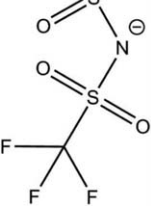
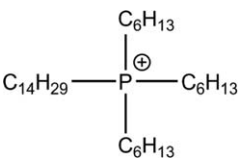
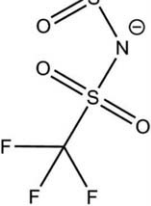
### Equipment

A synthetic apparatus with material balance is used for measurements of the solubility of CO<sub>2</sub> in the liquid phase. This device is detailed in previous works.<sup>25,28</sup> The system consists of a thermoregulated air bath containing a high pressure vessel to hold the CO<sub>2</sub> (loading side). The pressure inside the vessel is regulated with a Ruska pump (Model 2200) connected through a line filled with mercury. The temperature is measured with T type thermocouples (±1 K) controlled by a Sargent-Welch ST controller. The pressure is registered with a Heise Bourdon gauge (0–20 MPa with accuracies of ±0.02 MPa). The second side (cell side) is a water bath which controls the temperature of a calibrated volume 10-cm sapphire tube (Saphikon, maximum pressure 20 MPa) where the sample is loaded. A cathetometer (Titan Tool Supply Co., ±0.005 mm) is placed in front of the cell for registering the initial volume and volume change upon addition of CO<sub>2</sub> to the liquid mixture. The water bath is regulated with a quartz heater, controlled with a Sargent-Welch T controller. The temperature is measured with a platinum resistance thermometer (±0.3 K) connected to a Keithley meter (Model 2010, ±0.0001 mV, and ±0.0001 Ω) and the pressure inside the cell is registered with a Heise transducer (0–20 ± 0.01 MPa, Model 901A).

### Experimental procedures

For measuring the solubility of CO<sub>2</sub> in the liquid phase (single IL or toluene), the cell is loaded with 1–1.5 g of liquid, placed in a cell holder and connected to the lines. The cell side bath is filled with water, covering completely the cell, and the stirring system is activated to keep the set temperature constant. A small amount of CO<sub>2</sub> is added two or three times to the cell (0.1–0.2 MPa) to purge the remaining air in the lines and cell headspace. CO<sub>2</sub> is released until room pressure is reached. The initial height of the liquid is obtained with the cathetometer to calculate the initial volume with a previous obtained calibration curve (height vs. volume) for the cell. In the loading side, the temperature is kept at approximately 333 K and the pressure at 12.4 MPa. For the first run, a pressure of about 2 MPa of CO<sub>2</sub> is added to the cell and the pressure drop in the loading side is recovered to the initial value with the Ruska pump. The vapor-

**Table 1. Name, Structure, Abbreviation, and Purity of Ionic Liquids Used**

Name	Cation	Anion	Abbreviation	Purity
1-Hexyl-3-methylimidazolium bis(trifluoromethylsulfonyl) imide			[hmim][Tf <sub>2</sub> N]	Purity > 0.99 mass fraction [H <sub>2</sub> O] < 0.000326 mass fraction
1-Hexyl-3-methylpyridinium bis(trifluoromethylsulfonyl) imide			[hmpy][Tf <sub>2</sub> N]	Purity > 0.99 mass fraction [H <sub>2</sub> O] < 0.000394 mass fraction
Triethyloctyl phosphonium bis(trifluoromethylsulfonyl) imide			[P <sub>2228</sub> ][Tf <sub>2</sub> N]	Purity > 0.99 mass fraction [H <sub>2</sub> O] < 0.000601 mass fraction
Tetradecyltriethyl phosphonium bis(trifluoromethylsulfonyl) imide			[P <sub>66614</sub> ][Tf <sub>2</sub> N]	Purity > 0.99 mass fraction [H <sub>2</sub> O] < 0.000391 mass fraction

liquid equilibrium between CO<sub>2</sub> and the liquid is reached in the cell after stirring the liquid phase (15–30) min and confirmed by the constant pressure of the system. Finally, the new height of the liquid meniscus, the temperature and pressure of the cell, and the lines are recorded for equilibrium conditions. The procedure is repeated by systematically increasing the pressure of CO<sub>2</sub> in increments of 2 MPa until 8 MPa is reached. For calculating the moles of CO<sub>2</sub> in the vessel, lines, and cell headspace, the density of CO<sub>2</sub> is obtained with the Span–Wagner equation,<sup>38</sup> as done previously.<sup>25</sup>

The same procedure is followed to study the solubility of CO<sub>2</sub> in liquid mixtures; the only difference is the preparation of the sample. The cell is loaded with a mixture prepared by weighing the IL and the toluene and mixing them in a closed flask by stirring with a magnetic stir bar. The solubility procedure is analogous to the binary case, but the final pressure is that corresponding to the formation of a second liquid phase, that is, cloud point. The phase split is reached when the mixture becomes cloudy while stirring. An accurate value of the cloud point pressure is obtained by slowly adding CO<sub>2</sub> to the liquid mixture and visually detecting the cloudiness with a boroscope. Calculations are also performed with the Span–Wagner equation, assuming that the gas phase is pure CO<sub>2</sub>. In the literature,<sup>39,40</sup> compositions of toluene in the gas phase are no larger than 0.008 mole fraction at 313.15 K and 0.021 mole fraction at 333.15 K within the range of pressures studied. Thus, the density should not be modified significantly with the small amount of toluene dissolved in the CO<sub>2</sub> gas phase.

Propagation of error is obtained analogously as in previous work<sup>25,41</sup> for liquid compositions and molar volumes, with the only difference being the addition of the third component of the ternary system to this analysis. Using this method, the

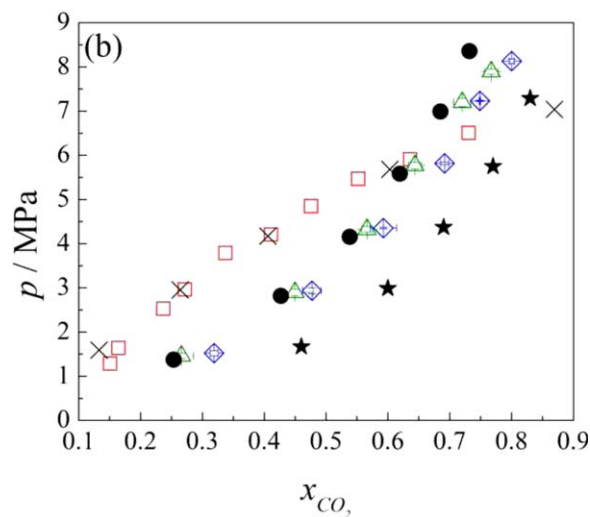
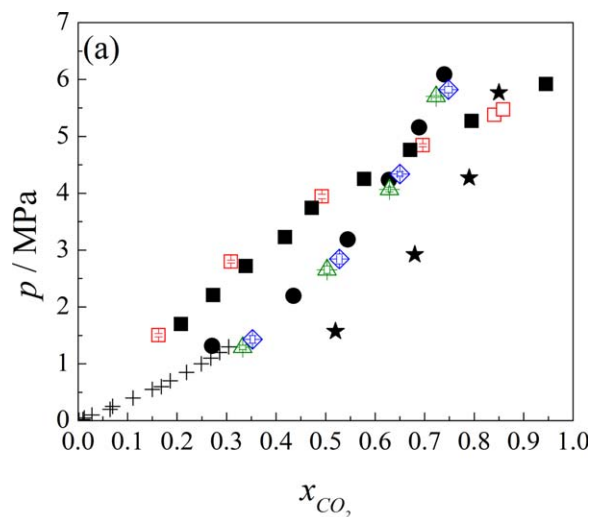
estimated error for the compositions is much smaller than the repeatability of the CO<sub>2</sub> solubility measurements. Therefore, the uncertainties of the compositions are calculated from the repeatability of points with similar pressures. For example, for duplicate or triplicate measurements at pressures that differ by less than 0.12 MPa we estimated the uncertainty in the CO<sub>2</sub> solubility as the standard deviation in the mole fraction for those replicates. After comparing repeatability between our data and reproducibility with literature values of the binary system CO<sub>2</sub> + toluene<sup>39,40,42</sup> and CO<sub>2</sub> + [hmim][Tf<sub>2</sub>N],<sup>24</sup> we estimate the uncertainty to be ±0.01 mole fraction of CO<sub>2</sub> for pressures over 3 MPa and ±0.02 mole fraction for pressures below 3 MPa for binary and ternary systems. This is true for both binary (IL + CO<sub>2</sub> and toluene + CO<sub>2</sub>) and ternary (IL + toluene + CO<sub>2</sub>) systems. The uncertainty in the molar volumes was calculated using the CO<sub>2</sub> solubility uncertainty and the uncertainty in reading the cathetometer.

## Results and Discussion

### Binary mixtures: Toluene + CO<sub>2</sub> and IL + CO<sub>2</sub>

The solubility of CO<sub>2</sub> was measured in the liquid phase of toluene at 298, 313, and 333 K in order to compare with literature data. We observed an average error of 1% (a maximum of ±0.02 mole fraction) when comparing our results with values shown in literature.<sup>39,40,42</sup>

The solubility of CO<sub>2</sub> in [hmim][Tf<sub>2</sub>N] and [P<sub>66614</sub>][Tf<sub>2</sub>N] at 298, 313, and 333 K and pressures to 11.56 MPa for [hmim][Tf<sub>2</sub>N] and 7.31 MPa for [P<sub>66614</sub>][Tf<sub>2</sub>N] have been measured previously by our research group<sup>24,25</sup> and others.<sup>43–45</sup> However, the solubility of CO<sub>2</sub> in [hmpy][Tf<sub>2</sub>N] has only been reported at 283, 298, and 323 K and pressures to 1.3 MPa.<sup>46</sup> Therefore, the new binary data measured here

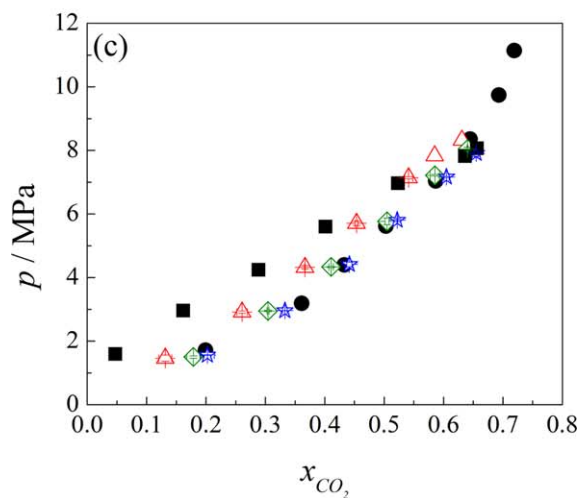
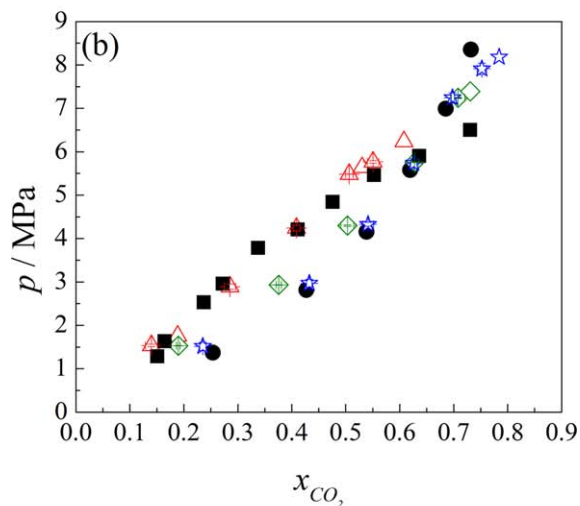
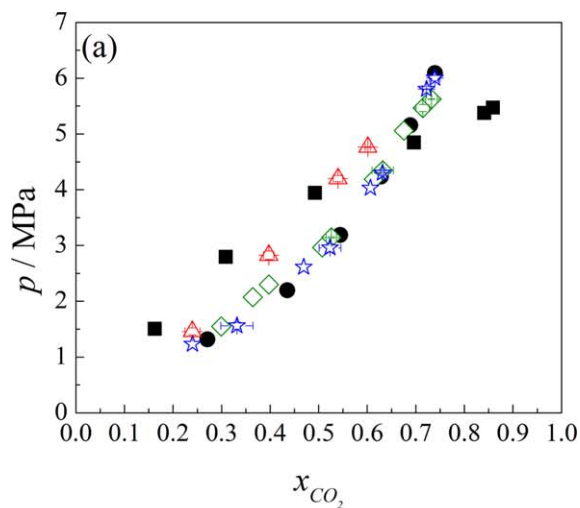


**Figure 2.** Solubility isotherms of CO<sub>2</sub> in  $\square$ , Toluene;  $\blacksquare$ , Toluene,<sup>42</sup>  $\times$ , Toluene at 311.26 K,<sup>39</sup>  $\bullet$ , [hmim][Tf<sub>2</sub>N]<sup>24</sup>;  $\triangle$ , [hmpy][Tf<sub>2</sub>N];  $+$ , [hmpy][Tf<sub>2</sub>N]<sup>46</sup>;  $\diamond$ , [P<sub>2228</sub>][Tf<sub>2</sub>N];  $\star$ , [P<sub>66614</sub>][Tf<sub>2</sub>N]<sup>25</sup> at (a) 298 K and (b) 313 K.

[Color figure can be viewed in the online issue, which is available at [wileyonlinelibrary.com](http://wileyonlinelibrary.com).]

includes equilibrium isotherms of CO<sub>2</sub> in [hmpy][Tf<sub>2</sub>N] and [P<sub>2228</sub>][Tf<sub>2</sub>N] at 298 and 313 K and pressures to 7.95 and 8.16 MPa, respectively. The new data and the data from the literature for the binary isotherms for all four ILs at 298 and 313 K are compared in Figure 2, along with the toluene/CO<sub>2</sub> binary data. The complete CO<sub>2</sub> solubility data for toluene, [hmpy][Tf<sub>2</sub>N], and [P<sub>2228</sub>][Tf<sub>2</sub>N] is shown in Supporting Information Tables S1–S3, respectively.

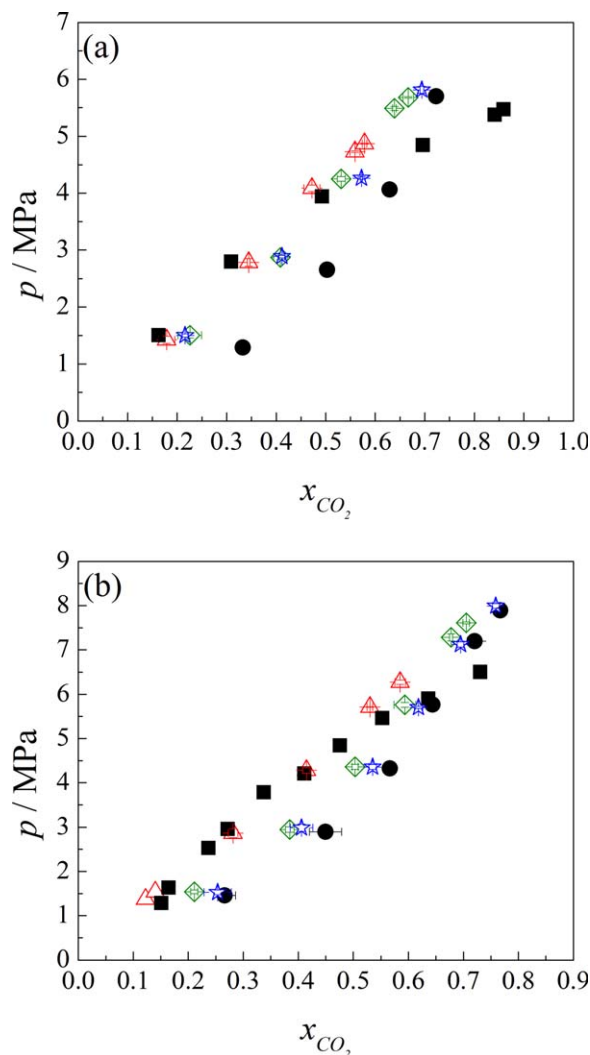
As is the case for [hmim][Tf<sub>2</sub>N] and [P<sub>66614</sub>][Tf<sub>2</sub>N], the solubility of CO<sub>2</sub> in [hmpy][Tf<sub>2</sub>N] and [P<sub>2228</sub>][Tf<sub>2</sub>N] is higher at lower temperatures and increases with increasing pressures, as expected. The solubility of CO<sub>2</sub> in toluene is lower than in all the ILs at lower pressures. However, the shape of the toluene isotherm is very different from the ILs and a crossover is observed around 0.7 mole fraction of CO<sub>2</sub>. When ILs are compared, [P<sub>66614</sub>][Tf<sub>2</sub>N] appears to have higher CO<sub>2</sub> solubility at all temperature and pressure conditions than the other ILs. It has been observed



**Figure 3.** Solubility isotherms of CO<sub>2</sub> in  $\blacksquare$ , Toluene;  $\triangle$ , 0.30 initial mole fraction of [hmim][Tf<sub>2</sub>N] in the [hmim][Tf<sub>2</sub>N] + toluene mixture;  $\diamond$ , 0.50 initial mole fraction of [hmim][Tf<sub>2</sub>N] in the [hmim][Tf<sub>2</sub>N] + toluene mixture;  $\star$ , 0.70 initial mole fraction of [hmim][Tf<sub>2</sub>N] in the [hmim][Tf<sub>2</sub>N] + toluene mixture;  $\bullet$ , [hmim][Tf<sub>2</sub>N]<sup>24</sup> at (a) 298 K, (b) 313 K and (c) 333 K.

[Color figure can be viewed in the online issue, which is available at [wileyonlinelibrary.com](http://wileyonlinelibrary.com).]





**Figure 4.** Solubility isotherms of  $\text{CO}_2$  in ■, Toluene;  $\Delta$ , 0.30 initial mole fraction of [hmpy][ $\text{Tf}_2\text{N}$ ] in the [hmpy][ $\text{Tf}_2\text{N}$ ] + toluene mixture;  $\diamond$ , 0.50 initial mole fraction of [hmpy][ $\text{Tf}_2\text{N}$ ] in the [hmpy][ $\text{Tf}_2\text{N}$ ] + toluene mixture;  $\star$ , 0.70 initial mole fraction of [hmpy][ $\text{Tf}_2\text{N}$ ] in the [hmpy][ $\text{Tf}_2\text{N}$ ] + toluene mixture; ●, [hmpy][ $\text{Tf}_2\text{N}$ ] at (a) 298 K and (b) 313 K.

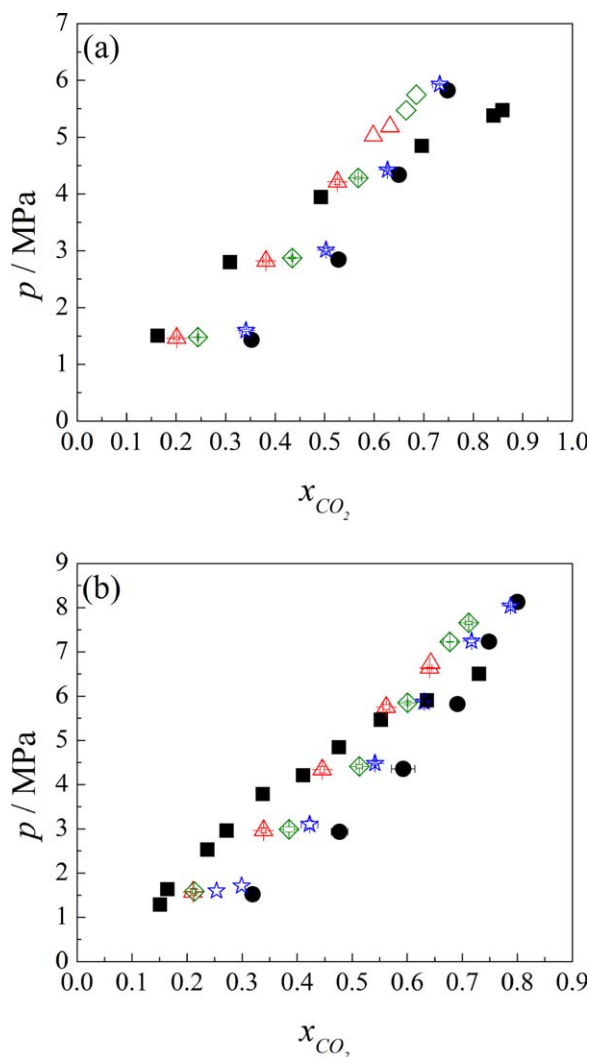
[Color figure can be viewed in the online issue, which is available at [wileyonlinelibrary.com](http://wileyonlinelibrary.com).]

previously<sup>25</sup> that this phosphonium-based IL has a remarkably higher capacity for  $\text{CO}_2$  than many other ILs with different anion-cation combinations. A reasonable explanation for the high  $\text{CO}_2$  solubility is the large free volume available in ILs made from the  $[\text{P}_{66614}]^+$  phosphonium cation, which contains four long organic chains. [hmim][ $\text{Tf}_2\text{N}$ ] and [hmpy][ $\text{Tf}_2\text{N}$ ] have very similar  $\text{CO}_2$  solubilities; in fact, based on data at pressures below 1.4 MPa, the Henry's law constants and enthalpy and entropy for  $\text{CO}_2$  dissolution are virtually identical for the two ILs.<sup>46,47</sup> This is not surprising as the ILs have the same anion and the same length alkyl chains on the cations. Both cations are nitrogen-containing aromatic rings. Only at 313 K and pressures over 7 MPa can one detect slightly higher  $\text{CO}_2$  solubility in [hmpy][ $\text{Tf}_2\text{N}$ ]. As shown in Figure 2, the high pressure  $\text{CO}_2$  solubility data taken here for [hmpy][ $\text{Tf}_2\text{N}$ ] is entirely consistent with the

low pressure literature values. For  $[\text{P}_{2228}][\text{Tf}_2\text{N}]$ , the  $\text{CO}_2$  solubilities are comparable to the values for [hmim][ $\text{Tf}_2\text{N}$ ] and [hmpy][ $\text{Tf}_2\text{N}$ ] at 298 K but are slightly higher at 313 K. The larger molar volume of the  $[\text{P}_{2228}]^+$  IL and greater flexibility of the alkyl chains of the phosphonium cation at higher temperatures than the more rigid cyclic imidazolium and pyridinium cations may be responsible for the higher solubility of  $\text{CO}_2$  at the higher temperature.

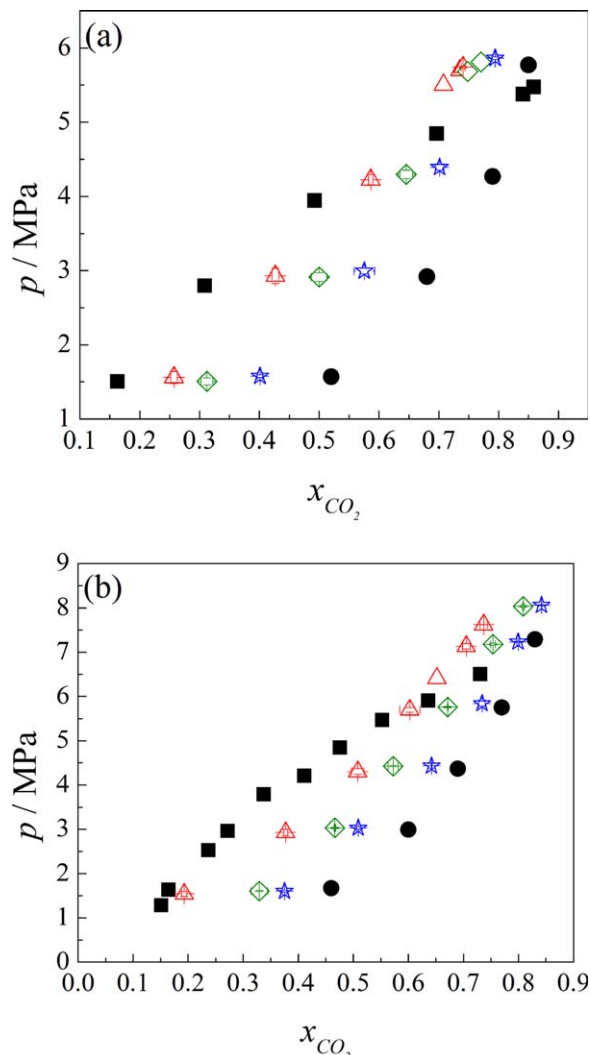
#### *Ternary mixtures: IL + Toluene + $\text{CO}_2$*

Here, we report three properties of the toluene + IL +  $\text{CO}_2$  systems. First, we show how the solubility of  $\text{CO}_2$  in the toluene + IL mixtures depends on temperature, pressure, and the relative amounts of toluene and IL in the liquid mixtures. Second, we report the pressures (and corresponding  $\text{CO}_2$  solubility) at which the liquid-liquid phase split (or cloud point)



**Figure 5.** Solubility isotherms of  $\text{CO}_2$  in ■, Toluene;  $\Delta$ , 0.30 initial mole fraction of  $[\text{P}_{2228}][\text{Tf}_2\text{N}]$  in the  $[\text{P}_{2228}][\text{Tf}_2\text{N}]$  + toluene mixture;  $\diamond$ , 0.50 initial mole fraction of  $[\text{P}_{2228}][\text{Tf}_2\text{N}]$  in the  $[\text{P}_{2228}][\text{Tf}_2\text{N}]$  + toluene mixture;  $\star$ , 0.70 initial mole fraction of  $[\text{P}_{2228}][\text{Tf}_2\text{N}]$  in the  $[\text{P}_{2228}][\text{Tf}_2\text{N}]$  + toluene mixture; ●,  $[\text{P}_{2228}][\text{Tf}_2\text{N}]$  at (a) 298 K and (b) 313 K.

[Color figure can be viewed in the online issue, which is available at [wileyonlinelibrary.com](http://wileyonlinelibrary.com).]



**Figure 6.** Solubility isotherms of CO<sub>2</sub> in: ■, Toluene; ▲, 0.30 initial mole fraction of [P<sub>66614</sub>][Tf<sub>2</sub>N] in the [P<sub>66614</sub>][Tf<sub>2</sub>N] + toluene mixture; ◇, 0.50 initial mole fraction of [P<sub>66614</sub>][Tf<sub>2</sub>N] in the [P<sub>66614</sub>][Tf<sub>2</sub>N] + toluene mixture; ☆, 0.70 initial mole fraction of [P<sub>66614</sub>][Tf<sub>2</sub>N] in the [P<sub>66614</sub>][Tf<sub>2</sub>N] + toluene mixture; ●, [P<sub>66614</sub>][Tf<sub>2</sub>N]<sup>25</sup> at (a) 298 K and (b) 313 K.

[Color figure can be viewed in the online issue, which is available at [wileyonlinelibrary.com](http://wileyonlinelibrary.com).]

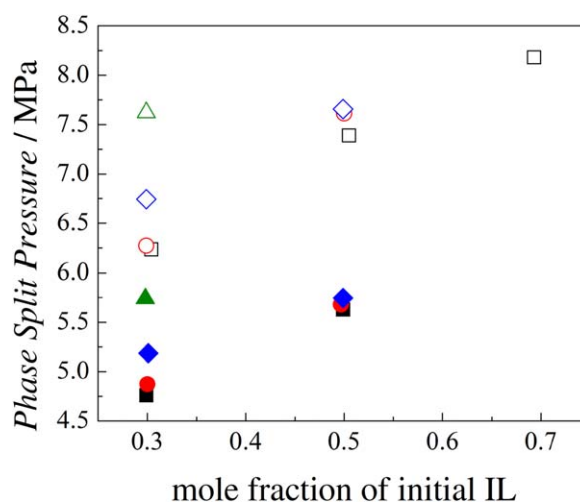
occurs for each IL as a function of temperature and the relative amounts of toluene and IL in the liquid phase. Finally, we report on the volume expansion that occurs as CO<sub>2</sub> is added to the toluene + IL mixtures and discuss how this influences the pressure (and CO<sub>2</sub> composition) at which the liquid-liquid phase split occurs. The [hmim][Tf<sub>2</sub>N] + toluene + CO<sub>2</sub> system was investigated at 298, 313, and 333 K. However, as no liquid-liquid phase split occurred at 333 K with [hmim][Tf<sub>2</sub>N] within the pressure range of our apparatus (up to 8 MPa), the [hmpy][Tf<sub>2</sub>N], [P<sub>2228</sub>][Tf<sub>2</sub>N], and [P<sub>66614</sub>][Tf<sub>2</sub>N] systems were studied only at 298 and 313 K. In each case, the maximum pressure investigated was either the pressure at which the liquid-liquid phase split was observed, the maximum pressure of the apparatus (8 MPa), or the pressure at which a liquid CO<sub>2</sub> phase is formed. This last situation is only encountered at

298 K, which is below the critical temperature of CO<sub>2</sub>. The vapor pressure of pure CO<sub>2</sub> at 298 K is roughly 6.2 MPa.

To determine the range of initial toluene + IL compositions that could be investigated, qualitative measurements of the solubility of toluene in each of the ILs were performed at room temperature. For [hmim][Tf<sub>2</sub>N], [hmpy][Tf<sub>2</sub>N], and [P<sub>2228</sub>][Tf<sub>2</sub>N], the estimated toluene solubility is between 0.80 and 0.85 mole fraction. Toluene is completely miscible with [P<sub>66614</sub>][Tf<sub>2</sub>N] at room temperature. High solubility of toluene has been measured previously in imidazolium ILs,<sup>48</sup> and this has been attributed to interactions of the highly electrostatic fields of the aromatic rings in both the IL and the toluene, as well as van der Waals interactions of the low polarity toluene with nonpolar chains on the cation of the IL.<sup>49,50</sup> The formation of clathrates by mixing [hmim][Tf<sub>2</sub>N] with toluene has been reported, as well.<sup>51</sup> The range of solubilities of toluene in the four ILs investigated here, including complete miscibility with [P<sub>66614</sub>][Tf<sub>2</sub>N], suggests that ILs + toluene exhibit normal liquid-phase dissolution, rather than the formation of any sort of specific stoichiometric complexation that could be characterized as a clathrate. Electrostatic interactions plus van der Waals forces can also account for the high solubility of toluene in [hmpy][Tf<sub>2</sub>N], due to the pyridinium cation's similarity with the imidazolium ring. In the case of phosphonium-based ILs, the high solubility of toluene is likely due to van der Waals interactions, which would increase with increasing alkyl chains length.<sup>52</sup> This is consistent with toluene being completely miscible with [P<sub>66614</sub>][Tf<sub>2</sub>N] but only partially miscible with [P<sub>2228</sub>][Tf<sub>2</sub>N]. Therefore, the initial compositions of the IL + toluene mixtures studied here were 0.30, 0.50, and 0.70 mole fraction IL. A single liquid phase was observed initially for all the temperatures investigated by using these compositions.

#### Solubility of CO<sub>2</sub> in mixtures of IL + toluene

The solubility of CO<sub>2</sub> in the mixtures of IL + toluene increases with increasing pressure, decreasing temperatures,



**Figure 7.** Phase split pressure at a determined initial composition of IL in the toluene + IL mixture for: ■, [hmim][Tf<sub>2</sub>N]; ●, [hmpy][Tf<sub>2</sub>N]; ◆, [P<sub>2228</sub>][Tf<sub>2</sub>N]; ▲, [P<sub>66614</sub>][Tf<sub>2</sub>N]. Filled symbols represent 298 K and open symbols 313 K.

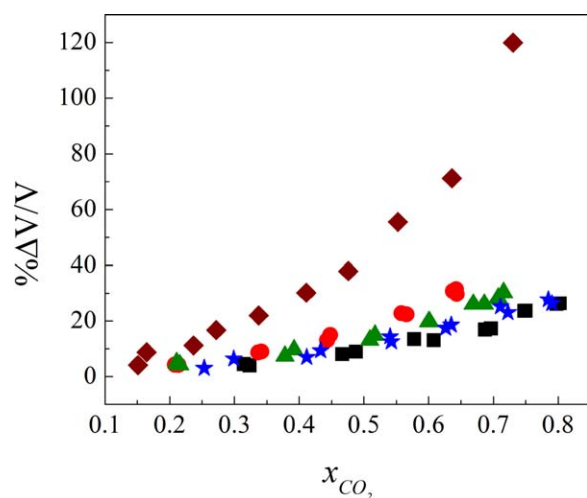
[Color figure can be viewed in the online issue, which is available at [wileyonlinelibrary.com](http://wileyonlinelibrary.com).]

and increasing amount of IL in the initial mixture. Figures 3–6 show the solubility of CO<sub>2</sub> in mixtures of toluene with [hmim][Tf<sub>2</sub>N], [hmpy][Tf<sub>2</sub>N], [P<sub>2228</sub>][Tf<sub>2</sub>N], and [P<sub>66614</sub>][Tf<sub>2</sub>N], respectively, at different initial liquid compositions, compared with the binary systems of CO<sub>2</sub> + IL and CO<sub>2</sub> + toluene. Supporting Information Tables S4–S7 show the complete solubility data measured for all these systems. The highest CO<sub>2</sub> solubility reported for each ternary isotherm is the cloud point, except in cases where no phase split had occurred even at the high pressure limit of the experimental apparatus.

Figures with the CO<sub>2</sub> uptake isotherms for the ternary systems can be found in Supporting Information Figures S1–S6. The figures compare the four different ILs at each temperature (298 and 313 K) and each initial IL + toluene composition (0.30, 0.50, and 0.70 mole fraction IL). The solubility of CO<sub>2</sub> in the [P<sub>66614</sub>][Tf<sub>2</sub>N] + toluene mixture is always higher than in the mixtures with the other three ILs. This is consistent with the binary results, where CO<sub>2</sub> had a higher solubility in pure [P<sub>66614</sub>][Tf<sub>2</sub>N] at both 298 and 313 K than in the other three pure ILs. For the ternaries, the higher solubility in the [P<sub>66614</sub>][Tf<sub>2</sub>N] + toluene mixtures is particularly obvious at the higher temperature—313 K. At 298 K, the solubility of CO<sub>2</sub> in the other three pure ILs was virtually identical. This is not the case for the mixtures with toluene. For all three initial IL + toluene compositions at 298 K, the CO<sub>2</sub> solubility is lowest in [hmpy][Tf<sub>2</sub>N] + toluene and highest in [hmim][Tf<sub>2</sub>N] + toluene (almost as high as in [P<sub>66614</sub>][Tf<sub>2</sub>N] + toluene for the 50/50 initial mixtures).

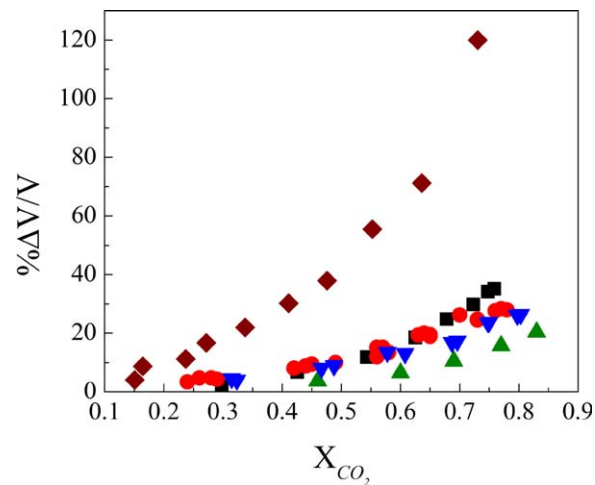
### Cloud points

Cloud points (the pressure at which a liquid-liquid phase split occurs) are observed in mixtures of [hmim][Tf<sub>2</sub>N] + toluene + CO<sub>2</sub> for all the initial liquid compositions at 313 K but only at 0.30 and 0.50 initial mole fraction of IL



**Figure 8.** Total volume expansion at 313 K of  $\blacklozenge$ , Toluene;  $\bullet$ , 0.30 mole fraction of initial [P<sub>2228</sub>][Tf<sub>2</sub>N] in the [P<sub>2228</sub>][Tf<sub>2</sub>N] + toluene mixture;  $\blacktriangle$ , 0.50 mole fraction of [P<sub>2228</sub>][Tf<sub>2</sub>N] in the [P<sub>2228</sub>][Tf<sub>2</sub>N] + toluene mixture;  $\star$ , 0.70 mole fraction of [P<sub>2228</sub>][Tf<sub>2</sub>N] in the [P<sub>2228</sub>][Tf<sub>2</sub>N] + toluene mixture;  $\blacksquare$ , [P<sub>2228</sub>][Tf<sub>2</sub>N] by adding CO<sub>2</sub>.

[Color figure can be viewed in the online issue, which is available at [www.interscience.wiley.com](http://www.interscience.wiley.com).]



**Figure 9.** Total volume expansion at 313 K of  $\blacklozenge$ , Toluene;  $\blacksquare$ , [hmim][Tf<sub>2</sub>N]<sup>24</sup>;  $\bullet$ , [hmpy][Tf<sub>2</sub>N];  $\blacktriangledown$ , [P<sub>2228</sub>][Tf<sub>2</sub>N];  $\blacktriangle$ , [P<sub>66614</sub>][Tf<sub>2</sub>N]<sup>25</sup> by adding CO<sub>2</sub>.

[Color figure can be viewed in the online issue, which is available at [www.interscience.wiley.com](http://www.interscience.wiley.com).]

at 298 K. No cloud points were obtained for this IL at 333 K at pressures below 8 MPa, so this temperature was not studied for the other IL mixtures. Cloud points are observed for initial IL + toluene mixtures containing both 0.30 and 0.50 mole fraction of IL with [hmpy][Tf<sub>2</sub>N] and [P<sub>2228</sub>][Tf<sub>2</sub>N] but only for an initial IL + toluene mixture containing 0.30 mole fraction of IL with [P<sub>66614</sub>][Tf<sub>2</sub>N]. This is true for both 298 and 313 K. Recall that at 313 K the highest pressure investigated was the pressure limit of the apparatus—8.2 MPa. However, at 298 K the highest pressure investigated was the pressure at which a liquid CO<sub>2</sub> phase appears—about 6 MPa. As shown in Figure 7, cloud point pressures are lower at lower temperature and lower initial mole fractions of IL in the IL + toluene liquid mixtures. It is observed that at the same initial composition of IL and different temperature, the same composition of CO<sub>2</sub> in the liquid mixture is required to induce a phase split for that IL. This behavior agrees with qualitative<sup>53,54</sup> and quantitative<sup>37</sup> ternary data for CO<sub>2</sub> + IL + methanol and CO<sub>2</sub> + IL + water systems shown by several authors. They show pressure-temperature diagrams at defined ternary system compositions, where the phase split pressure increases with increasing temperature until a tricritical point appears, that is, the high pressure and temperature point where the three phases coexist. Furthermore, previous work<sup>21,26–28</sup> has shown that cloud points are not observed when the initial composition of the polar organic compound is low in the IL phase. The same situation occurred with toluene mixed with the ILs studied here; a higher pressure is required to induce the second liquid phase when the amount of organic in the IL is small. Note that in all cases there is more than sufficient vapor phase volume (more than 50% of the volume in the cell) to allow the system to phase split if that were the thermodynamic equilibrium state.

In summary, one can most easily separate toluene from an IL using CO<sub>2</sub> to induce the formation of a second liquid phase, when the temperature is low (298 K) and there is a large amount of the organic dissolved in the IL. This scenario provides the lowest phase split pressures.



## Volume expansion

The liquid-liquid phase split occurs because the concentration of CO<sub>2</sub> in the liquid mixtures increases at a higher pressure, which increases the volume of the liquid phase. This expansion decreases the ability of the toluene and the IL to solvate each other, resulting in the phase split.

Total volume expansion<sup>55</sup> is calculated with Eq. 1, where  $V_L$  is the actual volume of the mixture when CO<sub>2</sub> is added and  $V_2$  is the initial volume of the IL or the IL + toluene mixture

$$\frac{\Delta V}{V} (\%) = \frac{V_L(T, P, x_1) - V_2(T, P_0)}{V_2(T, P_0)} \cdot 100 \quad (1)$$

The total volume expansion of toluene when adding CO<sub>2</sub> to the liquid phase is very high compared with ILs. This situation can be observed in Figure 8, where 0.70 mole fraction of CO<sub>2</sub> in toluene expands the solution to 100% more than its initial volume, while [P<sub>2228</sub>][Tf<sub>2</sub>N] at the same condition expands only 17%. The small expansion of IL + CO<sub>2</sub> systems can be attributed to the strong Coulombic forces that exert a large free energy penalty for separation of the cations and anions. Separation into two liquid phases, one rich in IL and the other rich in toluene, minimizes the free energy. Volume expansion depends mainly on the concentration of CO<sub>2</sub> in the liquid phase and it has a very small dependence on temperature.

From Figure 8, it is clear that mixtures with larger initial concentrations of toluene have higher volume expansions and these are the same mixtures that have lower cloud point pressures. Therefore, larger volume expansion of the ternary liquid mixture can be associated with milder conditions for obtaining a liquid-liquid phase split. This tendency is also observed in the other three ILs. Note that in the binary systems, larger volume expansion is observed for [hmim][Tf<sub>2</sub>N] and a smaller volume expansion is observed for [P<sub>66614</sub>][Tf<sub>2</sub>N] (Figure 9). This is consistent with the phase split pressure being lower for [hmim][Tf<sub>2</sub>N] than [P<sub>66614</sub>][Tf<sub>2</sub>N].

## Conclusions

Binary solubility isotherms of CO<sub>2</sub> were measured in toluene and two ILs for high pressure phase equilibrium, [hmpy][Tf<sub>2</sub>N] and [P<sub>2228</sub>][Tf<sub>2</sub>N]. These data were contrasted with ternary solubility isotherms of CO<sub>2</sub> in mixtures of toluene and four ILs, [hmim][Tf<sub>2</sub>N], [hmpy][Tf<sub>2</sub>N], [P<sub>66614</sub>][Tf<sub>2</sub>N], and [P<sub>2228</sub>][Tf<sub>2</sub>N], obtaining cloud points at determined conditions for all systems.

Solubility of CO<sub>2</sub> in liquid phases measured in this work increases with decreasing temperature and is enhanced by increasing the pressure of the system. The observation of cloud points in ternary systems is favorable when the concentration of toluene in the IL is high and when the temperature is low, because they are produced at lower pressures. This condition also coincides with a larger volume expansion of the liquid. Toluene can be separated from all the ILs studied in this work. A lower cloud point pressure is obtained when toluene is separated from [hmim][Tf<sub>2</sub>N], followed closely by [hmpy][Tf<sub>2</sub>N]. [P<sub>2228</sub>][Tf<sub>2</sub>N] has the same behavior as [hmim][Tf<sub>2</sub>N] and [hmpy][Tf<sub>2</sub>N] at 313 K but induces the phase split at higher pressure at 298 K. [P<sub>66614</sub>][Tf<sub>2</sub>N] only showed a cloud point at higher compositions of toluene in the initial mixture with IL and high pressures were required to induce a second liquid phase with this compound.

## Acknowledgment

The authors acknowledge the financial support from the Sustainable Energy Initiative (SEI) and the Center for Sustainable Energy at Notre Dame (cSEND).

## Literature Cited

1. Fredlake CP, Crosthwaite JM, Hert DG, Aki SNVK, Brennecke JF. Thermophysical properties of imidazolium-based ionic liquids. *J Chem Eng Data*. 2004;49(4):954–964.
2. Brennecke JF, Maginn EJ. Ionic liquids: innovative fluids for chemical processing. *AIChE J*. 2001;47(11):2384–2389.
3. Freire MG, Claudio AFM, Araujo JMM, Coutinho JAP, Marrucho IM, Lopes JNC, Rebelo LPN. Aqueous biphasic systems: a boost brought about by using ionic liquids. *Chem Soc Rev*. 2012;41(14):4966–4995.
4. Visser AE, Swatoski RP, Griffin ST, Hartman DH, Rogers RD. Liquid/liquid extraction of metal ions in room temperature ionic liquids. *Sep Sci Technol*. 2001;36(5–6):785–804.
5. Hoogerstraete TV, Onghena B, Binnemans K. Homogeneous liquid–liquid extraction of metal ions with a functionalized ionic liquid. *J Phys Chem Lett*. 2013;4:1659–1663.
6. Wei G-T, Yang Z, Chen C-J. Room temperature ionic liquid as a novel medium for liquid/liquid extraction of metal ions. *Anal Chim Acta*. 2003;488(2):183–192.
7. Fischer L, Falta T, Koellensperger G, Stojanovic A, Kogelnig D, Galanski M, Krachler R, Keppler BK. Ionic liquids for extraction of metals and metal containing compounds from communal and industrial waste water. *Water Res*. 2011;45(15):4601–4614.
8. Visser AE, Swatoski RP, Reichert WM, Mayton R, Sheff S, Wierzbicki A, Davis JH, Rogers RD. Task-specific ionic liquids incorporating novel cations for the coordination and extraction of Hg<sup>2+</sup> and Cd<sup>2+</sup>: synthesis, characterization, and extraction studies. *Environ Sci Technol*. 2002;36(11):2523–2529.
9. Cocalia VA, Holbrey JD, Gutowski KE, Bridges NJ, Rogers RD. Separations of metal ions using ionic liquids: the challenges of multiple mechanisms. *Tsinghua Sci Technol*. 2006;11(2):188–193.
10. Domańska U, Rękawek A. Extraction of metal ions from aqueous solutions using imidazolium based ionic liquids. *J Solut Chem*. 2009;38(6):739–751.
11. Huddleston JG, Rogers RD. Room temperature ionic liquids as novel media for “clean” liquid-liquid extraction. *Chem Commun*. 1998;(16):1765–1766.
12. Ha SH, Mai NL, Koo Y-M. Butanol recovery from aqueous solution into ionic liquids by liquid–liquid extraction. *Process Biochem*. 2010;45(12):1899–1903.
13. García S, Larriba M, García J, Torrecilla JS, Rodríguez F. Separation of toluene from n-heptane by liquid–liquid extraction using binary mixtures of [bpy][BF<sub>4</sub>] and [4bmpp][Tf<sub>2</sub>N] ionic liquids as solvent. *J Chem Thermodyn*. 2012;53:119–124.
14. Chapeaux A, Simoni LD, Ronan TS, Stadtherr MA, Brennecke JF. Extraction of alcohols from water with 1-hexyl-3-methylimidazolium bis(trifluoromethylsulfonyl)imide. *Green Chem*. 2008;10(12):1301–1306.
15. Brennecke JF, Gurkan BE. Ionic liquids for CO<sub>2</sub> capture and emission reduction. *J Phys Chem Lett*. 2010;1(24):3459–3464.
16. Ramdin M, de Loos TW, Vlucht TJH. State-of-the-art of CO<sub>2</sub> capture with ionic liquids. *Ind Eng Chem Res*. 2012;51(24):8149–8177.
17. Pereiro AB, Araújo JMM, Esperança JMSS, Marrucho IM, Rebelo LPN. Ionic liquids in separations of azeotropic systems – a review. *J Chem Thermodyn*. 2012;46:2–28.
18. Pereda S, Bottini S, Brignole E. Fundamentals of supercritical fluid technology. *Supercritical Fluid Extraction of Nutraceuticals and Bioactive Compounds*. CRC Press, Boca Raton, FL, USA, 2007:1–24.
19. Blanchard LA, Hancu D, Beckman EJ, Brennecke JF. Green processing using ionic liquids and CO<sub>2</sub>. *Nature*. 1999;399(6731):28–29.
20. Blanchard LA, Brennecke JF. Recovery of organic products from ionic liquids using supercritical carbon dioxide. *Ind Eng Chem Res*. 2001;40(1):287–292.
21. Scurto AM, Aki SNVK, Brennecke JF. CO<sub>2</sub> as a separation switch for ionic liquid/organic mixtures. *J Am Chem Soc*. 2002;124(35):10276–10277.
22. Blanchard LA, Gu Z, Brennecke JF. High-pressure phase behavior of ionic liquid/CO<sub>2</sub> systems. *J Phys Chem B*. 2001;105(12):2437–2444.



23. Cadena C, Anthony JL, Shah JK, Morrow TI, Brennecke JF, Maginn EJ. Why is CO<sub>2</sub> so soluble in imidazolium-based ionic liquids? *J Am Chem Soc.* 2004;126(16):5300–5308.
24. Aki SNVK, Mellein BR, Saurer EM, Brennecke JF. High-pressure phase behavior of carbon dioxide with imidazolium-based ionic liquids. *J Phys Chem B.* 2004;108(52):20355–20365.
25. Mejía I, Stanley K, Canales R, Brennecke JF. On the high-pressure solubilities of carbon dioxide in several ionic liquids. *J Chem Eng Data.* 2013;58(9):2642–2653.
26. Mellein BR, Brennecke JF. Characterization of the ability of CO<sub>2</sub> to act as an antisolvent for ionic liquid/organic mixtures<sup>†</sup>. *J Phys Chem B.* 2007;111(18):4837–4843.
27. Scurto AM, Aki SNVK, Brennecke JF. Carbon dioxide induced separation of ionic liquids and water. *Chem Commun.* 2003;(5):572–573.
28. Aki SNVK, Scurto AM, Brennecke JF. Ternary phase behavior of ionic liquid (il)–organic–CO<sub>2</sub> systems. *Ind Eng Chem Res.* 2006;45(16):5574–5585.
29. Zhang J, Li J, Zhao Y, Han B, Hou M, Yang G. Efficient separation of surfactant and organic solvent by CO<sub>2</sub>. *Chem Commun.* 2011;47(20):5816–5818.
30. Zhang Z, Wu W, Liu Z, Han B, Gao H, Jiang T. A study of triphasic behavior of ionic liquid-methanol-CO<sub>2</sub> systems at elevated pressures. *Phys Chem Chem Phys.* 2004;6(9):2352–2357.
31. Zhang Z, Wu W, Gao H, Han B, Wang B, Huang Y. Tri-phase behavior of ionic liquid-water-CO<sub>2</sub> system at elevated pressures. *Phys Chem Chem Phys.* 2004;6(21):5051–5055.
32. Chobanov K, Tuma D, Maurer G. High-pressure phase behavior of ternary systems (carbon dioxide + alkanol + hydrophobic ionic liquid). *Fluid Phase Equilib.* 2010;294(1–2):54–66.
33. Kühne E, Santarossa S, Perez E, Witkamp GJ, Peters CJ. New approach in the design of reactions and separations using an ionic liquid and carbon dioxide as solvents: phase equilibria in two selected ternary systems. *J Supercrit Fluids.* 2008;46(2):93–98.
34. Kühne E, Witkamp G-J, Peters CJ. High-pressure phase behavior of ternary mixtures with ionic liquids, part I: the system bmim[BF<sub>4</sub>]+4-isobutylacetophenone + CO<sub>2</sub>. *Green Chem.* 2008;10(9):929–933.
35. Kühne E, Perez E, Witkamp GJ, Peters CJ. Solute influence on the high-pressure phase equilibrium of ternary systems with carbon dioxide and an ionic liquid. *J Supercrit Fluids.* 2008;45(1):27–31.
36. Kroon MC, Florusse LJ, Kühne E, Witkamp G-J, Peters CJ. Achievement of a homogeneous phase in ternary ionic liquid/carbon dioxide/organic systems. *Ind Eng Chem Res.* 2010;49(7):3474–3478.
37. Kroon MC, Florusse LJ, Peters CJ. Phase behavior of the ternary 1-hexyl-3-methylimidazolium tetrafluoroborate + carbon dioxide + methanol system. *Fluid Phase Equilib.* 2010;294(1–2):84–88.
38. Span R, Wagner W. A new equation of state for carbon dioxide covering the fluid region from the triple-point temperature to 1100 K at pressures up to 800 MPa. *J Phys Chem Ref Data.* 1996;25(6):1509–1596.
39. Ng H-J, Robinson DB. Equilibrium-phase properties of the toluene-carbon dioxide system. *J Chem Eng Data.* 1978;23(4):325–327.
40. Tochigi K, Hasegawa K, Asano N, Kojima K. Vapor–liquid equilibria for the carbon dioxide + pentane and carbon dioxide + toluene systems. *J Chem Eng Data.* 1998;43(6):954–956.
41. Scurto AM. High-pressure phase and chemical equilibria of  $\beta$ -diketone ligands and chelates with carbon dioxide. Ph.D. Thesis, University of Notre Dame, Notre Dame, IN, USA, 2002.
42. Lay EN, Taghikhani V, Ghotbi C. Measurement and correlation of CO<sub>2</sub> solubility in the systems of CO<sub>2</sub> + toluene, CO<sub>2</sub> + benzene, and CO<sub>2</sub> + n-hexane at near-critical and supercritical conditions. *J Chem Eng Data.* 2006;51(6):2197–2200.
43. Ren W, Sensenich B, Scurto AM. High-pressure phase equilibria of {carbon dioxide (CO<sub>2</sub>) + n-alkyl-imidazolium bis(trifluoromethylsulfonyl)amide} ionic liquids. *J Chem Thermodyn.* 2010;42(3):305–311.
44. Raeissi S, Florusse L, Peters CJ. Scott–van Konynenburg phase diagram of carbon dioxide + alkylimidazolium-based ionic liquids. *J Supercrit Fluids.* 2010;55(2):825–832.
45. Yim J-H, Lim JS. CO<sub>2</sub> solubility measurement in 1-hexyl-3-methylimidazolium ([HMIM]) cation based ionic liquids. *Fluid Phase Equilib.* 2013;352:67–74.
46. Muldoon MJ, Aki SNVK, Anderson JL, Dixon JK, Brennecke JF. Improving carbon dioxide solubility in ionic liquids. *J Phys Chem B.* 2007;111(30):9001–9009.
47. Anderson JL, Dixon JK, Maginn EJ, Brennecke JF. Measurement of SO<sub>2</sub> solubility in ionic liquids. *J Phys Chem B.* 2006;110(31):15059–15062.
48. García S, Larriba M, García J, Torrecilla JS, Rodríguez F. Liquid-liquid extraction of toluene from heptane using 1-alkyl-3-methylimidazolium bis(trifluoromethylsulfonyl)imide ionic liquids. *J Chem Eng Data.* 2011;56(1):113–118.
49. Gutel T, Santini CC, Pádua AAH, Fenet B, Chauvin Y, Canongia Lopes JN, Bayard F, Costa Gomes MF, Pensado AS. Interaction between the  $\pi$ -system of toluene and the imidazolium ring of ionic liquids: a combined NMR and molecular simulation study. *J Phys Chem B.* 2008;113(1):170–177.
50. Hanke CG, Johansson A, Harper JB, Lynden-Bell RM. Why are aromatic compounds more soluble than aliphatic compounds in dimethylimidazolium ionic liquids? A simulation study. *Chem Phys Lett.* 2003;374(1–2):85–90.
51. Holbrey JD, Reichert WM, Nieuwenhuyzen M, Sheppard O, Hardacre C, Rogers RD. Liquid clathrate formation in ionic liquid-aromatic mixtures. *Chem Commun.* 2003;(4):476–477.
52. Liu X, Zhao Y, Zhang X, Zhou G, Zhang S. Microstructures and interaction analyses of phosphonium-based ionic liquids: a simulation study. *J Phys Chem B.* 2012;116(16):4934–4942.
53. Tuma D, Maurer G. Gas solubility in ionic liquids: mixed gases in pure ionic liquids and single gases in binary liquid mixtures. *Ionic Liquids: Science and Applications. ACS Symposium Series, Vol. 1117.* American Chemical Society, Washington DC, USA, 2012:10–217.
54. Maurer G, Tuma D. Gas solubility (and related high-pressure phenomena) in systems with ionic liquids. *Ionic Liquids: From Knowledge to Application. ACS Symposium Series, Vol. 1030.* American Chemical Society, Washington DC, USA, 2009:1–20.
55. De la Fuente Badilla JC, Peters CJ, de Swaan Arons J. Volume expansion in relation to the gas–antisolvent process. *J Supercrit Fluids.* 2000;17(1):13–23.

Manuscript received Dec. 7, 2014, and revision received Apr. 7, 2015.